Capture zones and scaling in homogeneous thin-film growth

P. A. Mulheran and J. A. Blackman
Department of Physics, The University of Reading, Whiteknights, Reading RG6 6AF, United Kingdom
(Received 25 October 1995; revised manuscript received 14 December 1995)

The capture zones for the islands in homogeneous thin-film growth simulations are studied. A complete condensation limit is used for the growth of dendritic and circular islands. The critical island sizes examined are $i=1$ in the former and $i=1,2,3$ in the latter case. It is found that the capture zones show scaling over all of the conditions and substrate coverages studied. In the high-temperature ($i>1$) regime this leads to the scaling of the island sizes themselves, and enables a semiempirical functional form derived for Voronoi networks to be assigned to the size distribution. In the low-temperature ($i=1$) regime the island size scaling with substrate coverage is only approximate and coincidental. These results show good agreement with previously published data from both experimental and computational studies.

I. INTRODUCTION

Interest in the process of submonolayer film growth has recently grown with the increasing applications of low-dimensional structures.[1] These include the epitaxial growth of semiconductors and metals[2] as well as nonepitaxial growth of metals on amorphous substrates.[3] Modeling of the evolution through computer simulation has led to a new understanding of the growth process, most notably in terms of scaling theory.[2,4–9] It is found that the scaled size distribution of the submonolayer islands has at least four universal curves, depending on the critical island size $i=0,1,2,3$. The critical island size is itself temperature dependent (i increases with temperature) and we shall consider $i=1,2,3$ in this paper. The observation of universal distributions applies to a range of simulation conditions[2] and to the experimental production of two-dimensional epitaxial films.[10] It is also found that the statistics of supported metal clusters follow a similar distribution to the low-temperature ($i=1$) case mentioned above.[11] Therefore key questions to be addressed by the modeling of the film growth is the precise nature of the scaling and the form of these ''universal'' curves. While an empirical form has been proposed for these,[12] we believe that the underlying cause of the scaling has been overlooked in the previous studies. It is the purpose of this paper to address the origins of the scaling in thin-film growth.

Scaling theories have been successfully applied to the dynamics of the island growth. Starting from appropriate rate equations the growth exponents for the island and monomer densities have been calculated.[4,5,9] This approach has also been extended to account for the dependence on the ratio $R=D/F$, where D is the monomer diffusion rate and F the monomer deposition rate.[2,7] In both cases satisfactory agreement with simulation results seem to have been achieved. However, this approach does not lead to a good understanding of the island size distribution functions. When the rate equations are numerically integrated the results do not compare well with simulation data, and crucially scaling behavior is not observed.[8] The reason for the poor results is easily understood. The rate equations themselves are mean field in nature, so that islands of the same size are calculated to all grow at the same rate. The calculated distribution of island sizes is broadened only by the varying nucleation times of islands. Thus if the islands were all nucleated simultaneously from randomly distributed defect sites the rate equations predict that they all would grow at identical rates and so remain equal in size throughout the evolution. Simulations of this ''heterogeneous'' nucleation process show that this is most definitely not the case.[13] The crucial ingredient missing from the rate equations is the variation in island environments due to the random positioning of the nucleation sites. The mean field rate equations alone cannot provide a complete description of film growth.

In an earlier paper we studied the heterogeneous growth process.[13] We observed that individual islands grow at a rate proportional to the size of their ''capture zones.'' An island's capture zone is that region of the substrate from which monomers are more likely to diffuse to this particular island than to any other in the system. It was demonstrated that the capture zones in the heterogeneous system are closely approximated by the Voronoi polygons for each nucleation site. The size distribution of the islands is then the same as that of the cell areas in the Voronoi network. Thus scaling in this system trivially follows since the capture zone network is static. Furthermore, a semiempirical form of the distribution function is known for random Voronoi networks, and this contains a convenient parametrization for the statistics relevant to the nucleation sites.

In this paper we have extended our studies of the capture zones and their influence on the island size scaling to the homogeneous growth process. In homogeneous systems islands nucleate when diffusing monomers come together to form stable nuclei. This may occur anywhere on the uncovered substrate throughout the film evolution, unlike the heterogeneous system mentioned above. The capture zone model of the island growth embodies the ingredient missing from the rate equations, namely, the variations in island environments. This model is not new, having been discussed by Venables and Ball in 1971.[14] These authors calculated the Voronoi capture zones of a few xenon crystals growing on graphite and found excellent correlation with their subsequent growth rates. Since then this approach appears to have been overlooked, yet we demonstrate in this paper that it lies at the heart of the scaling properties of the island arrays.

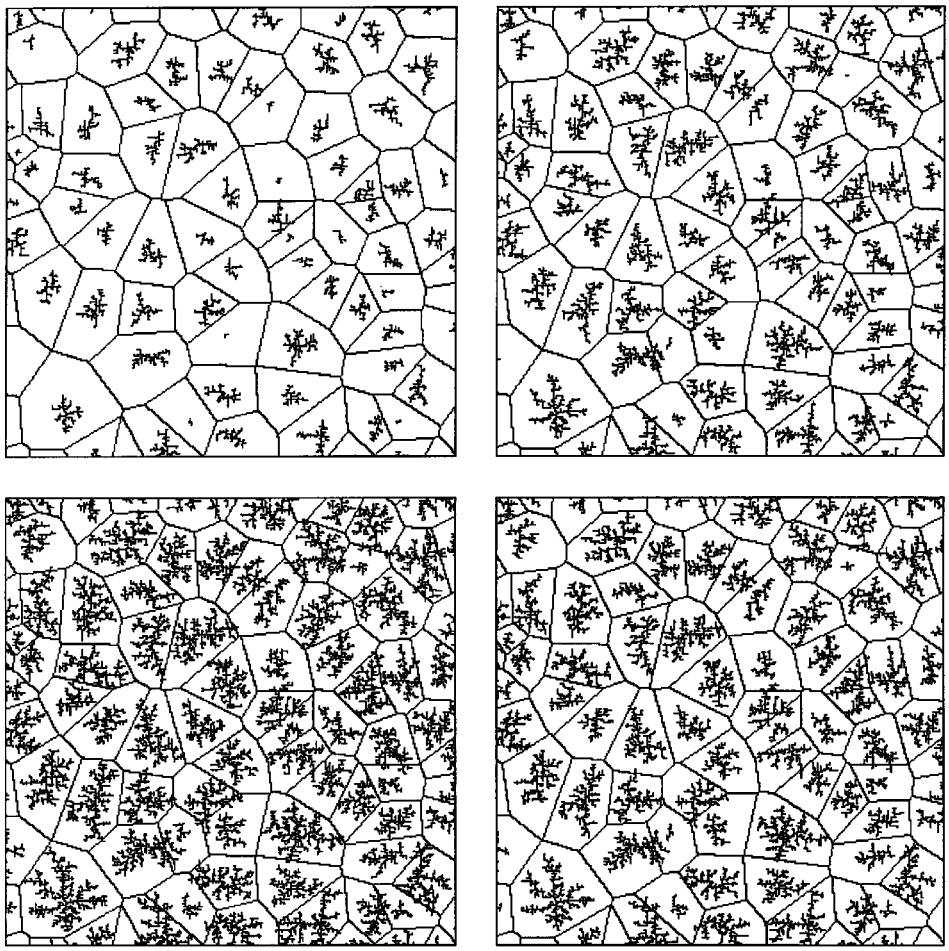

FIG. 1. Pictures of the evolving island structures in the simulation of dendritic islands. Starting from top left the coverage $\theta=5\%$, 10%, 15%, and 20% moving clockwise.

II. SIMULATION OF DENDRITIC ISLAND GROWTH

The simulation procedure we adopt here is similar to the one employed by Amar, Family, and Lam.[7] Monomers are randomly deposited at a rate F onto a square mesh, where they diffuse at a rate D by nearest-neighbor hops. Periodic boundary conditions are employed. When a monomer comes across another diffusing monomer as a nearest neighbor they both become fixed and form an island of size two. If a monomer encounters another that is already part of an existing island, it too freezes in place and joins the island. In this way the islands nucleate and grow as the simulation time t proceeds, with the coverage $\theta=Ft$. We are concerned here with $\theta\lesssim 30\%$ where the islands remain spatially distinct entities. Note that for simplicity we simulate "complete condensation,"[14] since evaporation from existing islands is not allowed. The critical island size i is 1, since islands of size $i+1=2$ are stable. This represents a low-temperature regime $k_BT<E$ where E is the pair bond energy.

Some snapshots of the developing islands are shown in Fig. 1, taking portions of the 500×500 mesh used. In these simulations $R=10^8$. The Voronoi polygons constructed from the positions of each island's nucleus are also shown in Fig. 1. This network is updated throughout the simulation whenever a new island nucleates. Note how the islands tend to grow into the shape of their Voronoi polygons. This is because the monomers causing the lateral growth of an island tend to arrive in proportion to the amount of vacant substrate between islands.

We wish to approximate the capture zone of an island by its Voronoi polygon. Since this may now change when a new island nucleates we must monitor its size throughout the deposition. From these data we *estimate* the size of the island, on the assumption that it grows at the rate F times its Voronoi polygon area, by integrating its growth rate over time. A comparison between this *estimate* and the *actual* is-

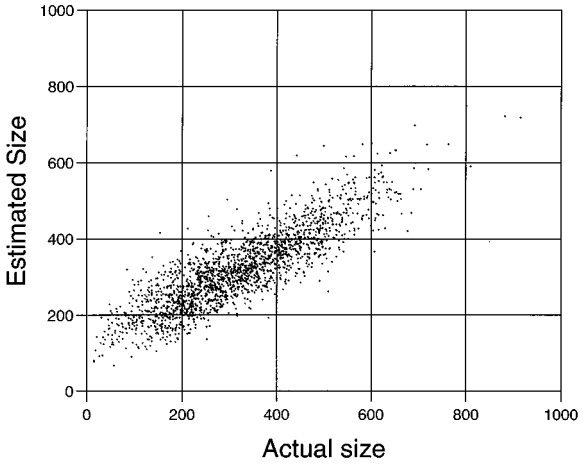

FIG. 2. The correlation between the actual island sizes and those estimated using the Voronoi polygon capture zones for the dendritic island simulation. The units for both axes are the number of monomers absorbed by the island.

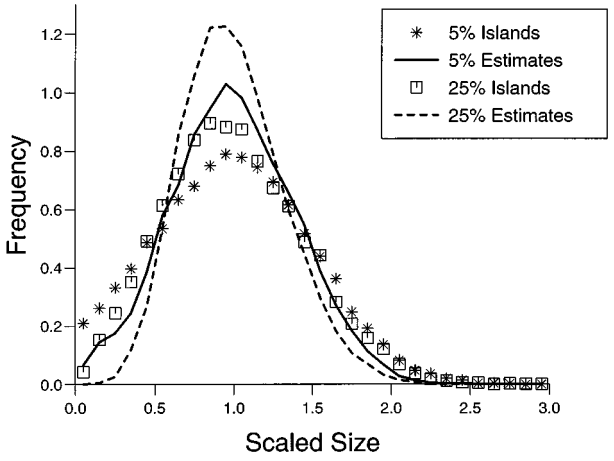

FIG. 3. Size distribution functions of the islands and the estimates at coverages $\theta=5\%$ and 25% for the dendritic island simulations. The sizes are scaled to the average in the array at each particular coverage, and the curves are all normalized to unit area. The data are the average from 100 simulations.

land size provides a measure of the accuracy of the model. The correlation in Fig. 2 shows that there is a large degree of agreement between the two. However, it is apparent that the Voronoi capture zone model tends to overestimate the size of small islands and underestimate the size of large ones. Hence while the Voronoi polygons provide a good first approximation to the islands' capture zones in this homogeneous growth process, they are not as satisfactory as in the heterogenous case.[13]

Returning to Fig. 1 it can been seen that by $\theta=20\%$ coverage the large islands tend to have outgrown their Voronoi polygons, spilling over into the polygons of smaller neighbors. This is consistent with the data of Fig. 2. The main failing of the Voronoi model is that the capture zone boundary is more likely to be equidistant from the edges of neighboring islands, not their centers. While this makes little difference to the heterogeneous growth process, in the present homogeneous situation it means that late nuclei are surrounded by islands of significant extent, which noticeably reduces their capture zones. The impact of this is demonstrated in Fig. 3, where the size distribution functions are plotted. Notice how the actual islands have a broader distribution than the simple Voronoi capture zone model predicts. It is apparent that a better description of the capture zones is required to achieve a thorough understanding of the island size distributions. Although alternatives of the Voronoi construction can be readily attempted, the dendritic nature of the islands studied here complicates the situation. We prefer instead to focus on the opposite extreme of compact circular islands, where the description of the capture zone is clear cut. This we do in the following section.

III. SIMULATION OF CIRCULAR ISLAND GROWTH

A. Low-temperature regime

The above simulation has been modified to the growth of circular islands. New islands now nucleate whenever two monomers coincide at the same site, so that the critical island size $i=1$ again. However, each island is now assumed to be a circle centered on its nucleation site, whose area is proportional to the number of monomers it has adsorbed. When a diffusing monomer encroaches within the area of an existing island it is absorbed and the area of the circle incremented by one unit. This represents an instantaneous relaxation of the island morphology to a compact and convex shape. We choose this shape to be circular both for computational convenience and for its merit as the antithesis of the dendritic islands used above. Another choice might have been a shape reflecting the symmetry of the underlying lattice;[15] however, we do not expect that this would have had any strong effect on the conclusions drawn from this section.

This is the form of the simulation we used to demonstrate the capture zone model in heterogeneous film growth.[13] The circular shape of the islands did not affect the arguments for using Voronoi polygons in that case. If we follow the polygons through the film evolution to estimate island sizes in the homogeneous situation the conclusions are identical to those of the dendritic simulations above, with curvature evident in the correlation between estimated and actual island sizes. However, it is easy to improve our approximations for the island capture zones with circular islands. When a new island nucleates, rather than employing the Voronoi condition of the zone boundaries being equidistant from the nucleation centers, we impose the condition that they are equidistant from island edges. This modified procedure can be shown to be preferable by using arguments based on the diffusion equation.[16] As a matter of computational convenience, we approximate the size of the neighbors of new nuclei as the average size in the array at that particular moment in the simulation. It will be shown below that this modified construction leads to much improved estimates of the islands' capture zones.

In Fig. 4 snapshots of this simulation with $R=10^8$ show the circular islands growing within their capture zones. The network of zone boundaries is only slightly different from that of the true Voronoi network, but note how the zone walls are slightly curved rather than straight lines. It is apparent how late nuclei (the very small islands in any given coverage) possess capture zones that are smaller than their Voronoi polygons, as required. By using these zones to predict the island sizes we obtain excellent correlation with the actual results as displayed in Fig. 5. The scatter here is probably due to the stochastic nature of the film growth, which leads to fluctuations in island sizes about the capture zone predictions. It is clear that the network of zones constructed here is an excellent representation of the true island capture zones.

Distributions of island sizes are shown in Fig. 6 along with those of the estimates from the capture zones. The agreement between them is very good, providing further validation of the capture zone model. Also shown in Fig. 6 are the distributions of the capture zone sizes found in the simulations. The islands themselves end up with a broader range of sizes due to the varying history of each island's environment, as discussed above. Note the occurrence of scaling in this figure, namely, the coincidence of the distributions at different coverages for both the island size data and the zones. We will discuss this further below.

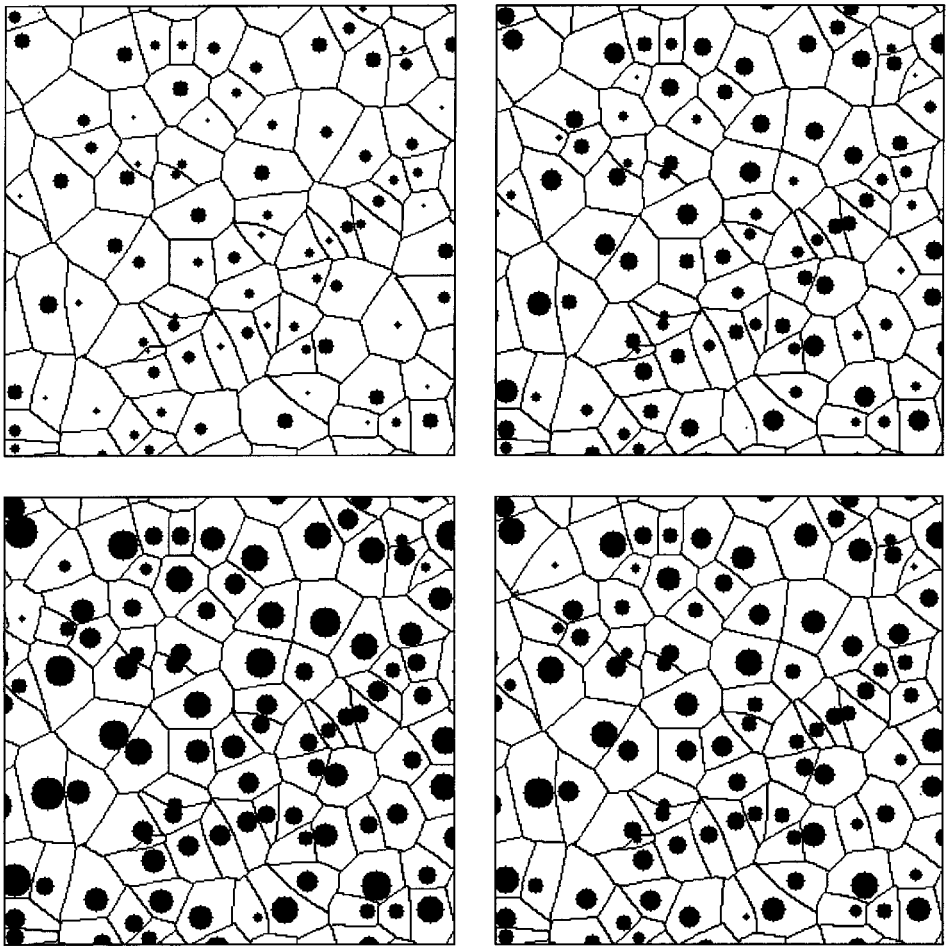

FIG. 4. Pictures of the evolving microstructure in the $i=1$ circular island simulations. As before the coverage $\theta=5\%$, 10%, 15%, and 20% starting top left and moving clockwise.

B. High-temperature regime

It has been observed that at high temperatures the distribution of island sizes is different from that at low temperatures.[2,10] The key effect of temperature appears to be to increase the critical island size i. To investigate this we simply modify the condition for nucleation in the simulation of circular islands. For a new island to nucleate we require $i+1$ monomers to coincide at the same site and at the same time. The remainder of the simulation algorithm remains unchanged. This affects the dynamics of the evolution in the following way. The probability of nucleating an island is proportional to the monomer density raised to the power $i+1$. Thus nucleation does not occur in the simulation until this density rises to much higher levels than in the $i=1$ case. For similar reasons, the period over which nucleation occurs

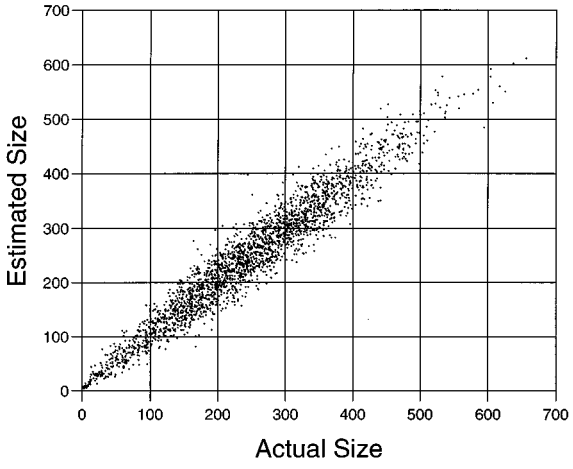

FIG. 5. The correlation between the actual island sizes and the estimates from the capture zones in the $i=1$ circular island simulations.

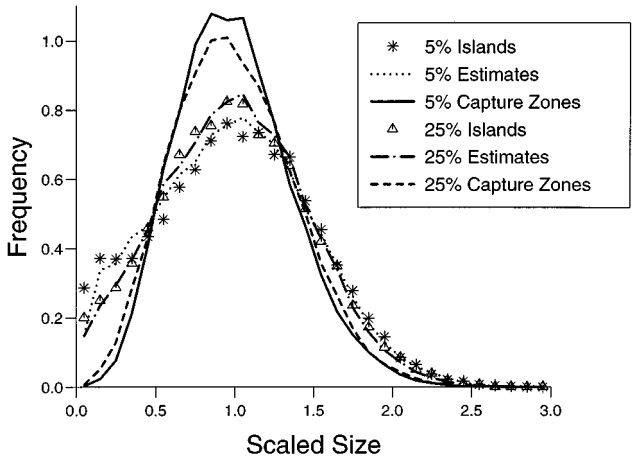

FIG. 6. The size distributions from the $i=1$ circular island simulations, comparing the actual islands, the estimates, and the capture zones at coverages $\theta=5\%$ and 25%. Again the sizes have been scaled and the curves normalized. The data are averaged from 100 simulations.

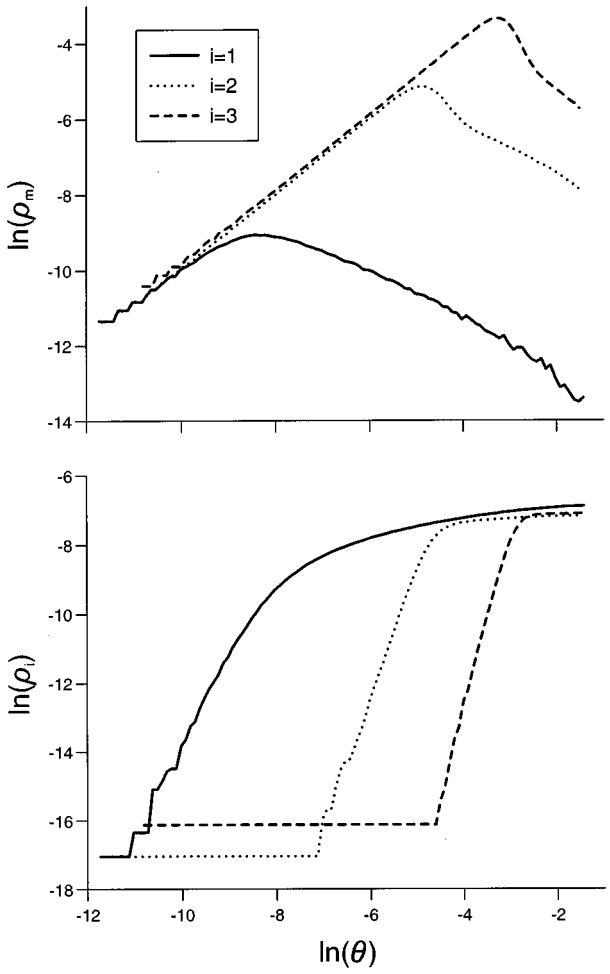

FIG. 7. The variation of the monomer and island densities ρ_m and ρ_i with coverage, for the circular island simulations with different critical island sizes $i=1,2,3$. The plateaus visible at low coverages are artifacts of the finite lattice sizes employed in the simulations.

is limited by the reduction in monomer density once several islands exist to absorb them. This behavior is displayed in Fig. 7 where the variation in both monomer and island density with coverage θ is shown. The $i=1$ case (with $R=10^8$) shows substantial nucleation virtually throughout the simulation. However, the $i=2$ simulation (with $R=10^6$) has a rather limited period of nucleation, and the $i=3$ case (with $R=10^5$) is even more extreme.

The shorter period of significant nucleation for the $i=2$ simulation is reflected in the size distributions shown in Fig. 8. Once again the distribution of the estimates from the capture zones agree very well with the island size data. The capture zone distributions remain rather similar to those in the $i=1$ case. It is now notable that the island sizes show much less broadening than before (see Fig. 6). The almost contemporaneous nucleation of the islands means that their capture zones remain more or less unchanged throughout the film growth, leading to island sizes in proportion to their current capture zone areas. Thus the high-temperature $i>1$ regime bears strong resemblance to the heterogeneous growth situation.

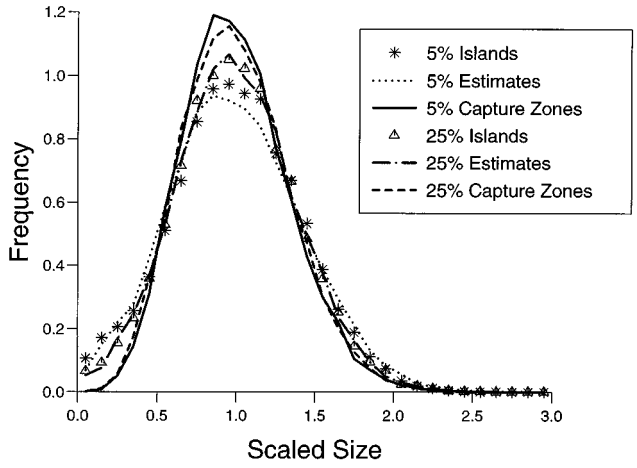

FIG. 8. The scaled size distributions from 100 runs of the $i=2$ circular island simulations.

IV. DISCUSSION

We have shown how the capture zone structure underpins the island size distributions in various circumstances. Now the capture zone size distribution itself displays scaling behavior as shown in Fig. 9. This distribution is very similar to that of a Voronoi network with a hard-disk exclusion providing a minimum separation between nuclei.[17] The distribution $F(y)$ of scaled Voronoi polygon areas y obeys the following semiempirical form:

$$F(y)=\frac{\beta^{\beta}}{\Gamma(\beta)}y^{\beta-1}\exp(-\beta y). \tag{1}$$

The parameter $\beta=3.61$ for the random network with no exclusion.[18,19] We have found that when one creates Voronoi networks with exclusion, then $F(y)$ still describes the distribution of polygon areas if one employs an increased value of β.[13] In fact β increases monotonically with the degree of exclusion, and so is a useful empirical parameter for the networks. In the case of heterogeneous nucleation, we had complete freedom to choose the degree of exclusion in the

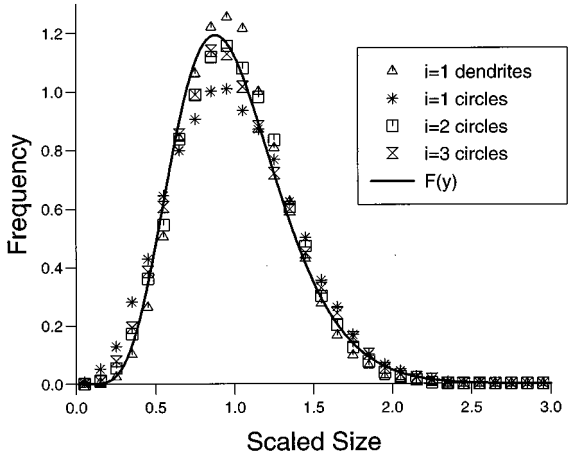

FIG. 9. The scaled size distributions for the capture zones from the different simulations discussed in this paper, compared to the curve $F(y)$ of Eq. (1).

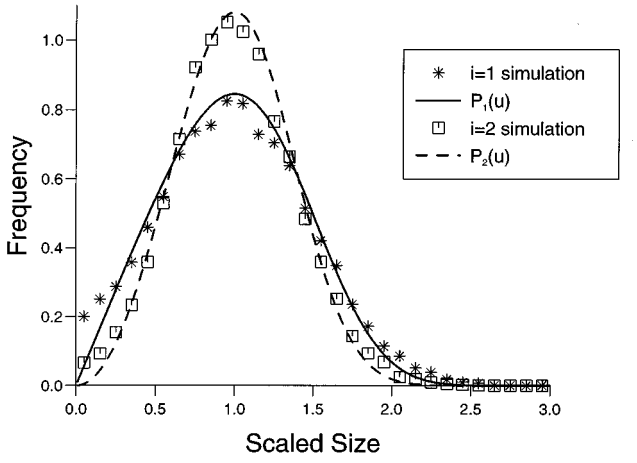

FIG. 10. Comparison between the empirical curves of Amar and Family (Ref. 12), Eq. 2, and the island size distributions from simulations of the homogeneous nucleation of circular islands with $i=1,2$. These data are taken from Figs. 6 and 8, respectively, with $\theta=25\%$.

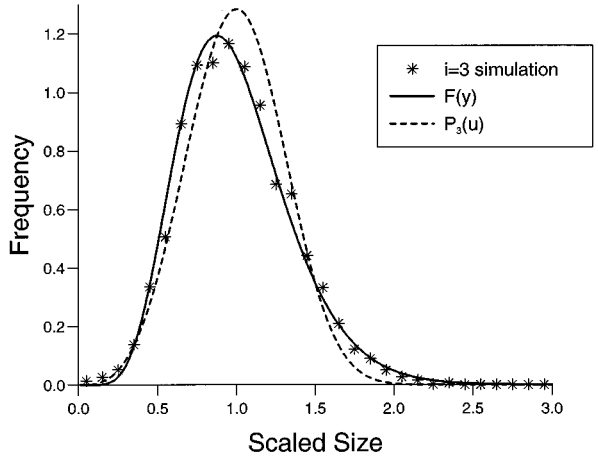

FIG. 11. Comparisons between the $i=3$ simulation results and the curves $F(y)$ and P_3.

nuclei arrangements.[13] In the present homogeneous case, the exclusion arises naturally and is not imposed externally. Now the curves in Fig. 9 are well approximated by $F(y)$ with $\beta \simeq 8$, and we have found that this corresponds to a Voronoi network where 30% of initially random points are eliminated from the system by the nearest-neighbor exclusion.[20] Why does such a distribution of nuclei arise naturally in the homogeneous growth process? The answer lies in the monomer exclusion zone that surrounds each existing island.[2,4] This inhibits new nucleation in the immediate vicinity of existing islands, thereby keeping the islands separated.

Given the scaling of the capture zones, scaling of the island sizes in the high-temperature $i>1$ regime in different systems is no surprise. Indeed the curve $F(y)$ is a useful functional form for comparing these systems. While it is semiempirical in nature it does at least originate from consideration of the growth mechanism. However, in the low-temperature $i=1$ regime island size scaling is more of a surprise. It is clear why the distributions are broadened beyond the capture zones, but not obvious why the extent of this broadening is the same for different coverages. The scaling apparent in Fig. 6 for the circular islands is probably coincidental rather than mechanistic. Returning to the distributions from the dendritic islands in Fig. 3, there is clearly no exact scaling. This departure from scaling is also apparent in the data published by Amar, Family, and Lam[7] from their simulations of dendritic islands. Thus there is evidence to support the idea that the scaling observed in low-temperature systems is accidental, notwithstanding the scaling of the underlying capture zones.

Finally one must address whether the simulations studied here are really representative of the other systems that have been studied. The simplest way to test this is to compare our distributions with those published in the literature by overlaying the graphs with suitable magnifications. We find extremely good agreement between the distributions in the following cases: Fig. 3 and the data of Amar, Family, and Lam for dendritic islands;[7] Fig. 6 ($i=1$ circles), the low-temperature simulation results of Ratsch *et al.*[2] and the experimental data of Stroscio and Pierce;[10] the $i=2$ data in Fig. 8 and the high-temperature results of the two studies just cited.[2,10] Additionally, we can provide a more quantitative comparison by utilizing the empirical curves suggested by Amar and Family.[12] They find that their simulation data are well represented by the curves

$$P_i(u)=C_i u^i \exp(-i a_i u^{1/a_i}), \tag{2}$$

where i is the critical island size ($i=1,2,3$) and u is the scaled island size. The constants C_i and a_i are determined by the usual sum rules for a scaled distribution function. In Fig. 10 the $\theta=25\%$ data from Figs. 6 and 8 ($i=1,2$, respectively) is plotted along side these curves. Excellent agreement is observed, despite the different simulation algorithms used in the other work. The only point of departure concerns the small size frequencies for the $i=1$ case. Once again this is a feature apparent in other published simulation results. However, Amar and Family find in their extensive computational studies[12] that the distribution does eventually converge to the linear form shown at small island size, though high values of the diffusion to deposition ratio R and large coverage θ are required.

The $i=3$ case is slightly less clear cut. In Fig. 11, we plot the island size distribution at $\theta=25\%$ from a simulation with $i=3$ and $R=10^6$. We find excellent agreement with the capture zone distribution which is $F(y)$ of Eq. (1). This is precisely the behavior we expect following the above discussion of minimal broadening at high temperatures, and we see no reason for different behavior in our simulations at even higher temperatures and critical island sizes $i>3$. However, it is also apparent that the empirical curve P_3 of Eq. (2) is slightly, but noticeably, different to $F(y)$ and so our results for $i=3$ are not the same as those of Amar and Family.[12] This could be due to the scatter in the $i=3$ data of Ref. 12, which is approximately $\pm 10\%$ at the maximum, although

this explanation is not very convincing when one overlays the curve $F(y)$ onto the published figure. Another possible explanation lies in the inherently different simulation algorithms employed, and that more subtle mechanisms than those considered here might have a measurable effect on the high-temperature island size distributions. Further investigation on this point is desirable.

From the above, largely favorable, comparisons we draw the conclusion that the explanation offered here for the scaling behavior of our simulations is sufficiently general in its approach to describe film growth over a range of different conditions. While we have concentrated on two-dimensional island growth, generalization to systems where islands grow in three dimensions is clearly straightforward.

[1] A.-L. Barabási and H. E. Stanley, in *Fractal Concepts in Surface Growth* (Cambridge University Press, Cambridge, 1995).
[2] C. Ratsch, A. Zangwill, P. Šmilauer, and D. D. Vvedensky, Phys. Rev. Lett. **72**, 3194 (1994).
[3] Shi Xu, B. L. Evans, D. I. Flynn, and C. En, Thin Solid Films **238**, 13 863 (1994).
[4] J. A. Venables, Philos. Mag. **27**, 697 (1973).
[5] J. A. Blackman and A. Wilding, Europhys. Lett. **16**, 115 (1991); J. Phys. A **27**, 725 (1994).
[6] M. C. Bartelt and J. W. Evans, Phys. Rev. B **46**, 12 675 (1992).
[7] J. G. Amar, F. Family, and P.-M. Lam, Phys. Rev. B **50**, 8781 (1994).
[8] G. S. Bales and D. C. Chrzan, Phys. Rev. B **50**, 6057 (1994).
[9] F. Family and P. Meakin, Phys. Rev. A **40**, 3836 (1989).
[10] J. A. Stroscio and D. T. Pierce, Phys. Rev. B **49**, 8522 (1994).
[11] J. A. Blackman and P. A. Mulheran, in *Electronic, Optoelectronic and Magnetic Thin Films* edited by J. M. Marshall, N. Kirov, and A. Vavrek (Research Studies Press, Taunton, 1995), p. 227.
[12] J. G. Amar and F. Family, Phys. Rev. Lett. **74**, 2066 (1995).
[13] P. A. Mulheran and J. A. Blackman, Philos. Mag. Lett. **72**, 55 (1995).
[14] J. A. Venables and D. J. Ball, Proc. R. Soc. London A **332**, 331 (1971).
[15] G. T. Barkema, O. Biham, M. Breeman, D. O. Boerma, and G. Vidali, Surf. Sci. Lett. **306**, L569 (1994).
[16] J. A. Blackman and P. A. Mulheran (unpublished).
[17] D. L. Weaire and N. Rivier, Contemp. Phys. **23**, 59 (1984).
[18] D. L. Weaire, J. P. Kermode, and J. Wejchert, Philos. Mag. B **53**, L101 (1986).
[19] P. A. Mulheran, Philos. Mag. Lett. **66**, 219 (1992).
[20] The algorithm used to create the nearest-neighbor exclusion is as follows. N sites are chosen at random to be potential Voronoi centers. The center with the smallest nearest-neighbor distance in the system is then removed, and this step is repeated until the desired percentage of centers have been excluded. The Voronoi construction is then made for the surviving centers. With $0.3N$ removed (as cited in the text) we find that the area of the exclusion zone around each center is approximately $0.14\bar{a}$, where $\bar{a}$ is the average Voronoi polygon area in the generated network.